Biomedical Microdevices (2019) 21: 31
https://doi.org/10.1007/s10544-019-0358-0

Engineered microscale hydrogels for drug delivery, cell therapy, and sequencing

Marissa E. Wechsler[1,2] · Regan E. Stephenson[3] · Andrew C. Murphy[2,4] · Heidi F. Oldenkamp[2,4] · Ankur Singh[3,5,6] · Nicholas A. Peppas[1,2,4,7,8]

Published online: 23 March 2019

Abstract
Engineered microscale hydrogels have emerged as promising therapeutic approaches for the treatment of various diseases. These microgels find wide application in the biomedical field because of the ease of injectability, controlled release of therapeutics, flexible means of synthesis, associated tunability, and can be engineered as stimuli-responsive. While bulk hydrogels of several length-scale dimensions have been used for over two decades in drug delivery applications, their use as microscale carriers of drug and cell-based therapies is relatively new. Herein, we critically summarize the fundamentals of hydrogels based on their equilibrium and dynamics of their molecular structure, as well as solute diffusion as it relates to drug delivery. In addition, examples of common microgel synthesis techniques are provided. The ability to tune microscale hydrogels to obtain controlled release of therapeutics is discussed, along with microgel considerations for cell encapsulation as it relates to the development of cell-based therapies. We conclude with an outlook on the use of microgels for cell sequencing, and the convergence of the use of microscale hydrogels for drug delivery, cell therapy, and cell sequencing based systems.

Keywords Cell therapy · Drug delivery · Hydrogels · Sequencing

1 Introduction

Hydrogels are three-dimensional, hydrophilic networks, produced from crosslinked homopolymers, copolymers, or macromers (Peppas 1986; Slaughter et al. 2009). These hydrophilic polymer networks have a large affinity for water, but are insoluble due to the presence of either chemical or physical crosslinks which provide structure and physical integrity throughout the network (Peppas et al. 2000, 2006). Both synthetic and natural polymers have been used to synthesize hydrogels. They include polyacrylates (such as, poly(2-hydroxyethyl methacrylate)), poly(ethylene glycol), poly(vinyl alcohol), gelatin, alginate, chitosan, fibrin, collagen, in addition to many others (Suri and Schmidt 2009; Nikkhah et al. 2012; Morelli et al. 2016; Neves et al. 2017; Wang et al. 2018). Examples of common synthetic polymers are shown in Fig. 1. Hydrogels made from these materials are attractive for many biomedical applications due to their biocompatibility and water content that simulates natural tissues.

✉ Nicholas A. Peppas
peppas@che.utexas.edu

[1] Department of Biomedical Engineering, The University of Texas at Austin, Austin, TX, USA

[2] Institute for Biomaterials, Drug Delivery, and Regenerative Medicine, The University of Texas at Austin, Austin, TX, USA

[3] Meinig School of Biomedical Engineering, Cornell University, Ithaca, NY, USA

[4] McKetta Department of Chemical Engineering, The University of Texas at Austin, Austin, TX, USA

[5] Sibley School of Mechanical and Aerospace Engineering, Cornell University, Ithaca, NY, USA

[6] Englander Institute for Precision Medicine, Weill Cornell Medical College, New York, NY, USA

[7] Division of Molecular Pharmaceutics and Drug Delivery, College of Pharmacy, The University of Texas at Austin, Austin, TX, USA

[8] Department of Surgery and Perioperative Care, and Department of Pediatrics, Dell Medical School, The University of Texas at Austin, Austin, TX, USA

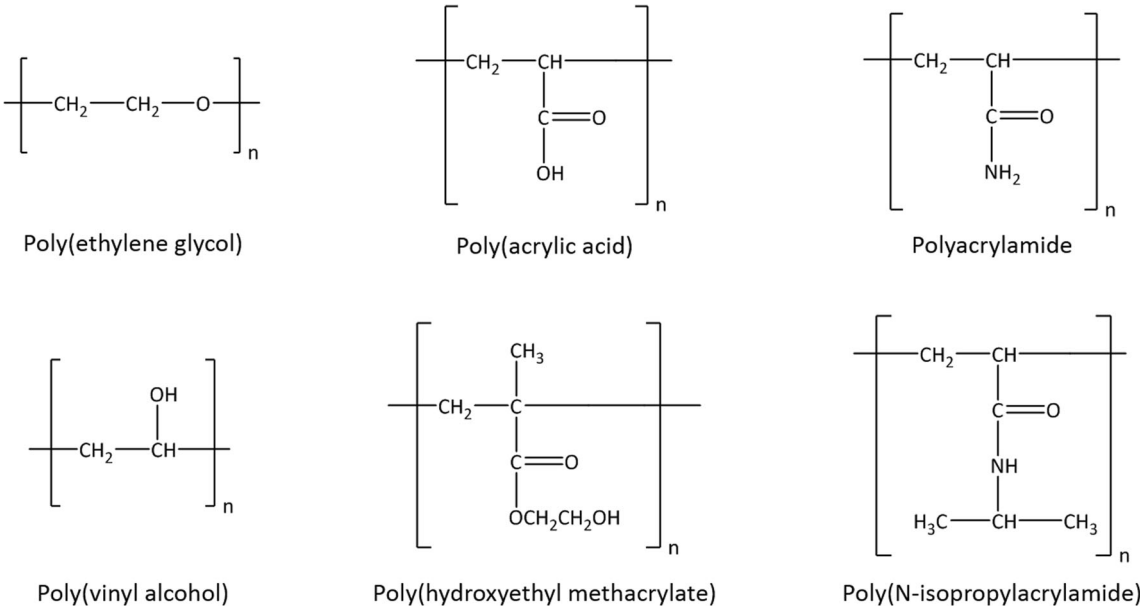

Fig. 1 Representative chemical structures of synthetic polymers used for biomedical applications

2 Hydrogel fundamentals

2.1 Network structure and characterization

Networks and the associated hydrogels can be neutral, cationic, anionic, or ampholytic as dictated by the pendant groups incorporated into the polymer backbone. Ionic gels (whether cationic, anionic, or amphoteric) in aqueous solvents are generally charged (to a certain extent) due to the protonation or deprotonation of charged pendant groups at the pH of the solvent. The extent to which charged pendant groups are either protonated or deprotonated can be controlled by adjusting the pH of the solvent. Hydrogels which deprotonate in the absorbed solvent are anionic, while hydrogels that protonate are cationic.

In anionic hydrogels, the quantity of deprotonated, negatively-charged pendant groups exceeds uncharged pendant groups when the pH of the solvent is greater than the pKa of the polyacid (commonly carboxylic acids). In contrast, cationic hydrogels have positively-charged, protonated pendant groups that are present at higher concentrations compared to neutral pendant groups when the pH is below the pKa of the conjugate polyacid (commonly protonated amines). As a result of varying pendant group incorporation into the hydrogel backbone, these networks can demonstrate environmentally responsive swelling behaviors. Factors which can affect hydrogel swelling in aqueous solutions include pH (Fig. 2a) and ionic strength (Fig. 2b); their influence is indicated by the general dependence shown in the Fig. 2.

Several quantitative parameters can be used to describe the network structure of hydrogels. The most important parameters used for hydrogel characterization include the polymer volume fraction in the swollen state ($\upsilon_{2,s}$), the number average molecular weight between crosslinks ($\overline{M_c}$), and the molecular distance between two consecutive crosslinks, otherwise known as mesh size (ξ). These related parameters can be predicted theoretically and determined experimentally. However, the two most prominent methods used to obtain these parameters which describe the hydrogel network structure are derived from equilibrium swelling theory and rubber elasticity theory (Lowman et al. 2004).

2.2 Equilibrium swelling theory

The Flory–Rehner theory (Flory and Rehner 1943), used for the analysis of neutral hydrogels, describes swelling by indicating that crosslinked polymer gels immersed in a fluidic environment will reach equilibrium as a subject of two opposing forces: (i) the thermodynamic force via mixing and (ii) the retractive force of the polymer chains.

Analytically, this is expressed in terms of the Gibbs free energy, shown in Eq. 1. Here, $\Delta G_{elastic}$ represents the contribution to the Gibbs free energy due to elastic, retractive forces inside the hydrogel, and ΔG_{mixing} is the Gibbs free energy change due to the compatibility of the polymer and the solvent.

$$\Delta G_{total} = \Delta G_{elastic} + \Delta G_{mixing} \tag{1}$$

Differentiation of Eq. 1 with respect to the moles of solvent, while maintaining constant pressure and temperature, results in Eq. 2. Here, μ_1 and $\mu_{1,o}$ are the chemical potential of the solvent in the hydrogel and pure solvent, respectively. At equilibrium, the difference between the two chemical potentials (solvent outside and inside of the hydrogel) must be

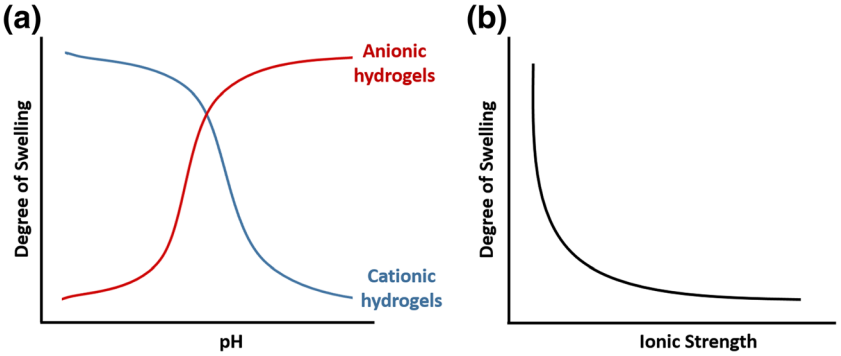

Fig. 2 Swelling behavior of ionizable hydrogels in aqueous solutions. **a** Cationic hydrogels remain in a swollen state at low pH and transition into a collapsed state at high pH, while anionic hydrogels are collapsed at low pH and swell at high pH. **b** Swelling of hydrogels decreases with increasing ionic strength. Figure adapted from (Culver and Peppas 2017)

equal to zero, and therefore, differences in chemical potential due to elastic forces and mixing must balance.

$$\mu_1 - \mu_{1,o} = \Delta\mu_{elastic} + \Delta\mu_{mixing} \tag{2}$$

The theory of rubber elasticity can be used to determine the change in chemical potential due to elastic forces, and moreover, lead to an expression (Eq. 3) to obtain the average molecular weight between crosslinks, $\overline{M_c}$, if the neutral hydrogel is prepared in the absence of solvent. In equation 3, $\overline{M_n}$ is the molecular weight of the polymer chains prepared under identical conditions but in the absence of the crosslinking agent, $\bar{v}$ is the specific volume of the polymer, V_1 is the molar volume of the swelling agent (water), and $\upsilon_{2,s}$ represents the polymer volume fraction in the swollen state. It must be noted that this equation was developed for crosslinked systems with tetrafunctional crosslinks.

$$\frac{1}{\overline{M_c}} = \frac{2}{\overline{M_n}} - \frac{\left(\frac{\bar{v}}{V_1}\right)\left[\ln\left(1-\upsilon_{2,s}\right) + \upsilon_{2,s} + \chi_1\upsilon_{2,s}^2\right]}{\left(\upsilon_{2,s}^{1/3} - \frac{\upsilon_{2,s}}{2}\right)} \tag{3}$$

This theory was further modified by Peppas and Merrill (Peppas and Merrill 1977) for hydrogels prepared in the presence of water (Equation 4). This adaption modifies the change in chemical potential due to elastic forces to take into account the volume fraction density of the chains during crosslinking. In Equation 4, $\upsilon_{2,r}$ denotes the polymer volume fraction in the relaxed state (the state of the polymer immediately after crosslinking), while $\upsilon_{2,s}$ represents the polymer volume fraction in the swollen state in water.

$$\frac{1}{\overline{M_c}} = \frac{2}{\overline{M_n}} - \frac{\left(\frac{\bar{v}}{V_1}\right)\left[\ln\left(1-\upsilon_{2,s}\right) + \upsilon_{2,s} + \chi_1\upsilon_{2,s}^2\right]}{\upsilon_{2,r}\left[\left(\frac{\upsilon_{2,s}}{\upsilon_{2,r}}\right)^{1/3} - \left(\frac{\upsilon_{2,s}}{2\upsilon_{2,r}}\right)\right]} \tag{4}$$

The presence of ionic moieties within hydrogels adds complexity to the swelling analysis by incorporating a term to account for the total change in Gibbs free energy due to the ionic properties of the network, ΔG_{ionic}. This modification is shown in Equation 5.

$$\Delta G_{total} = \Delta G_{elastic} + \Delta G_{mixing} + \Delta G_{ionic} \tag{5}$$

Again, upon differentiating Equation 5 with respect to the moles of solvent molecules, while maintaining constant pressure and temperature, Equation 6 can be obtained. Here, while the expression is similar to that of Equation 2, the term $\Delta\mu_{ionic}$ represents the change in chemical potential due to the ionic nature of the hydrogel.

$$\mu_1 - \mu_{1,o} = \Delta\mu_{elastic} + \Delta\mu_{mixing} + \Delta\mu_{ionic} \tag{6}$$

A more complex equation was derived by Brannon-Peppas and Peppas (Brannon-Peppas and Peppas 1990) for the swelling behavior of ionic hydrogels. For anionic (Equation 7) and cationic (Equation 8) hydrogels, two separate expressions were obtained. Use of these expressions for analysis of the average molecular weight between crosslinks now requires information and numerical values of the ionic strength (I) and the equivalent dissociation constants (K_a and K_b for acids and bases, respectively).

$$\frac{V_1}{4I}\left(\frac{\upsilon_{2,s}^2}{\bar{v}^2}\right)\left(\frac{K_a}{10^{-pH}+K_a}\right)^2 = \left[\ln\left(1-\upsilon_{2,s}\right) + \upsilon_{2,s} + \chi_1\upsilon_{2,s}^2\right] + \left(\frac{V_1}{\bar{v}\overline{M_c}}\right)\left(1-\frac{2\overline{M_c}}{\overline{M_n}}\right)\upsilon_{2,r}\left[\left(\frac{\upsilon_{2,s}}{\upsilon_{2,r}}\right)^{1/3} - \left(\frac{\upsilon_{2,s}}{2\upsilon_{2,r}}\right)\right] \tag{7}$$

$$\frac{V_1}{4I}\left(\frac{\upsilon_{2,s}^2}{\bar{v}^2}\right)\left(\frac{K_b}{10^{pH-14}+K_a}\right)^2 = \left[\ln\left(1-\upsilon_{2,s}\right) + \upsilon_{2,s} + \chi_1\upsilon_{2,s}^2\right] + \left(\frac{V_1}{\bar{v}\overline{M_c}}\right)\left(1-\frac{2\overline{M_c}}{\overline{M_n}}\right)\upsilon_{2,r}\left[\left(\frac{\upsilon_{2,s}}{\upsilon_{2,r}}\right)^{1/3} - \left(\frac{\upsilon_{2,s}}{2\upsilon_{2,r}}\right)\right] \tag{8}$$

For solute (drug, peptide, protein, therapeutic agent) transport, the primary mechanism of transport or release is diffusion through the molecular space between polymer chains, often referred to as "molecular pores" or mesh. Depending on the size of the pores, hydrogels can be classified either as nonporous, microporous, or macroporous. In addition, the type and structure of crosslinking throughout the hydrogel can greatly affect its properties (such as porosity) through factors such as entanglements, hydrogen bonding, ionic bonding, crystallites, and covalent bonding.

The porosity of hydrogels can be defined by the structural parameter (ξ), the mesh size. The mesh size, or correlation length, determines the average linear distance between crosslinks as shown in Equation 9. In this expression, the unperturbed end-to-end distance between neighboring crosslinks is $(\bar{r_o}^2)^{1/2}$ (a known value) and the extension ratio (α) can be determined using Equation 10 from the polymer volume fraction in the swollen state ($\upsilon_{2,\,s}$). However, mesh size can be predicted without the unperturbed distance using Equation 11 if the values of certain parameters are available or can be determined: the bond length of the polymer backbone (l), the characteristic ratio (C_n), the average molecular weight between crosslinks ($\overline{M_c}$), the polymer volume fraction in the swollen state ($\upsilon_{2,\,s}$), and the molecular weight of repeating units (M_r).

$$\xi = \alpha\left(\bar{r_o}^2\right)^{1/2} \tag{9}$$

$$\alpha = \upsilon_{2,s}^{1/3} \tag{10}$$

$$\xi = \upsilon_{2,s}^{-1/3}\left(\frac{2C_n\overline{M_c}}{M_r}\right)^{1/2} l \tag{11}$$

The ability to tailor the molecular structure of networks and the thermodynamic/swelling behavior of hydrogels using several key parameters enables tuning of their diffusive, responsive, and mechanical properties (Peppas et al. 2006). These parameters are the polymer volume fraction in the swollen state ($\upsilon_{2,\,s}$), the average molecular weight between crosslinks ($\overline{M_c}$), and the mesh size (ξ).

2.3 Solute diffusion from hydrogels

Understanding solute transport is likely the single most important design parameter for hydrogels used as drug carriers. Since solute transport within hydrogels is primarily based on diffusion, Fick's law of diffusion can be used to describe this phenomenon shown in Equations 12 and 13. Here, c_i represents the concentration, j_i indicates the mass flux of solute i, and $D_{i,\,p}$ is the diffusion coefficient of solute i in the polymer matrix, p.

$$j_i = -D_{i,p}\frac{dc_i}{dx} \tag{12}$$

$$\frac{\partial c_i}{\partial t} = D_{i,p}\frac{\partial^2 c_i}{\partial x^2} \tag{13}$$

It is important to note that several assumptions have been incorporated into the equations above. First, these equations describe solute release from a carrier of a thin, planar geometry; although equivalent equations for solute release from carries with a variety of other geometries have been derived (Crank 1975).

In addition, in the form of Fick's law shown above, the diffusion coefficient is assumed to be independent of concentration. Thus, to improve the predictive power of Fickian diffusion, a concentration-dependent diffusion coefficient is used and can be written as Equation 14. In Equation 14, $D_{i,\,p}(c_i)$ is the concentration-dependent diffusion coefficient, and its form is dependent upon characteristics of the polymer matrix (Peppas and Narasimhan 2014).

$$\frac{\partial c_i}{\partial t} = \frac{\partial}{\partial z}\left(D_{i,p}(c_i)\frac{\partial c_i}{\partial x}\right) \tag{14}$$

In typical solute eluting systems, diffusion commonly dictates distribution of solutes throughout hydrogels and delivery to its surrounding environment. Drug release from these swelling-controlled systems (where solute release is mediated by the inward flux of solvent molecules and subsequent swelling of the polymer matrix) can be predicted via a power law relation derived by Korsmeyer and Peppas (Korsmeyer et al. 1983), shown in Equation 15. Here, M_t and M_∞ are the cumulative amounts of drug released at time t and equilibrium, respectively, k is a constant dictated by the structural and geometric information about the matrix, and n is indicative of the drug release mechanism. Release by Fickian diffusion using Equation 15 is approximated with $n = 0.5$.

$$\frac{M_t}{M_\infty} = kt^n \tag{15}$$

3 Methods of synthesizing microscale hydrogels

Polymeric microgels have emerged as a popular alternatives to bulk hydrogels because of their ease of injectability, size control, immunoisolation, and enhanced nutrient transport. Microscale hydrogels can be tuned to release encapsulated drugs and proteins at controlled rates based on diffusion through the hydrogel network, hydrolytic degradation of

polymer network, or stimuli-responsive swelling of the network. In contrast to bulk hydrogels, the microscale diameter of microgels also maximizes transport of oxygen and nutrients into and out of hydrogels, which is specifically beneficial to encapsulated cells. For applications in drug delivery and cell encapsulation, approaches for the synthesis of controlled hydrogel architectures at the microscale level have been developed. Figure 3 summarizes some of the most prevalent techniques used to synthesize polymeric microscale hydrogels for biomedical applications. Methods like microfluidics allow for the production of microdroplet carriers that are well-suited for drug delivery applications (Foster et al. 2017). In contrast, lithography offers improved control over the three-dimensional nanoscale structure of the hydrogel which has been exploited for drug delivery applications (Gratton et al. 2007; Caldorera-Moore et al. 2011) and microscale patterning of cell-laden hydrogels for tissue engineering applications (Suri and Schmidt 2009; Mironi-Harpaz et al. 2015). In each case, the hydrogel precursor is chosen to produce the desired network properties and can be a monomer solution or uncrosslinked polymer combined with a crosslinking agent. Cells or therapeutic agents can then be included in the pre-polymer solution, allowing for simultaneous encapsulation, or in the case of drug delivery applications, the drug can be loaded into the carrier post-synthesis through complexation with functional groups such as carboxylate anions.

3.1 Microfluidics

Droplet-producing microfluidic devices are emerging as the method of choice for microgel fabrication because they are easily customizable for the design requirements of the microgel application. These devices work by sectioning off pre-gel materials in an oil emulsion phase and typically achieved using a T-junction (Tan and Takeuchi 2007) or flow-focusing design (Headen et al. 2014, 2018a; Chen et al. 2016b; Foster et al. 2017; Lienemann et al. 2017; Zhang et al. 2018). By adjusting the flow rate ratios of input fluids, microgels of varying sizes and dispersity can be produced at a rapid rate with the fastest production of monodisperse microgels occurring during the jetting phase (Headen et al. 2014; Zhang et al. 2018). Microgel production rate has been reported between 250 and 1200 Hz depending on particle diameter (Griffin et al. 2015). Through adopting a device design with parallel flow focusers, this rate has been increased by up to 6-fold (Headen et al. 2018a), thereby reducing the time cells interact with pre-gel components and increasing throughput capacity. Headen et al. demonstrated that parallel microfluidic devices can increase microgel production rate by 600% with minimal impact on the size or polydispersity compared to single nozzle microfluidic devices.

Successful microfluidic-directed gelation of PEG-based macromers specifically, PEG-maleimide (Headen et al.

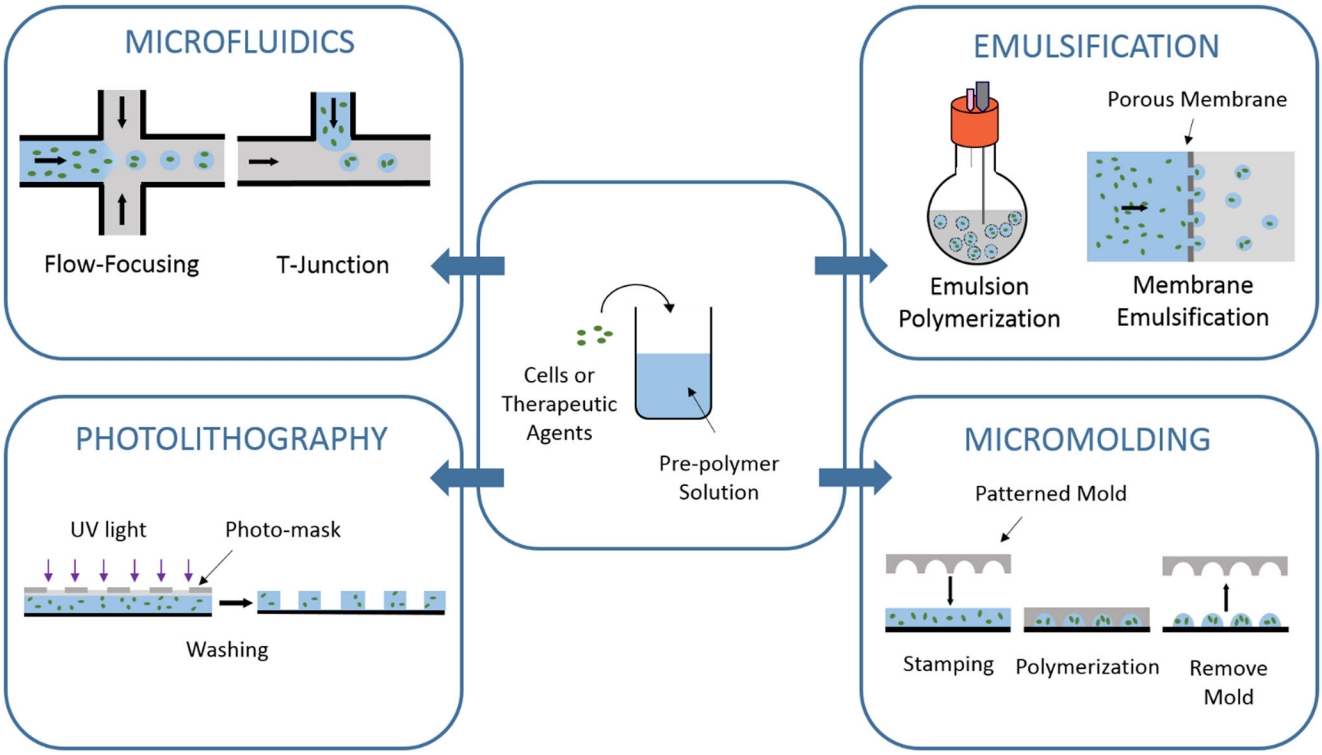

Fig. 3 Schematic of microscale hydrogel synthesis techniques. A pre-polymer solution containing the desired components of the hydrogel network is combined with cells or therapeutic agents for simultaneous encapsulation. Microstructures are formed using techniques such as microfluidics, emulsification, photolithography, or micromolding, and the network is crosslinked to form microgels

2014, 2018a, 2018b; Foster et al. 2017), PEG-vinylsulfone (Allazetta et al. 2013; Lienemann et al. 2017), PEG-acrylates (Choi et al. 2016), alginate (Tan and Takeuchi 2007; Hirama et al. 2012; Kim et al. 2014; Chen et al. 2016a; Mao et al. 2017; Zhang et al. 2018), and methacrylated gelatin (Rossow et al. 2012; Lee and Cha 2018) have been established to date. These biomaterial systems vary in crosslinking chemistry, pH requirements, and number of precursor solutions required before gelation, all of which drive design requirements of the microfluidic device for the microgel on-chip gelation process.

Combination of a macromer and a crosslinking agent, for example in the case of PEG-maleimide, requires fast on-chip combination to avoid premature crosslinking (Foster et al. 2017), or a diffusive design when the crosslinking agent is small enough to allow diffusion through macromer on-chip (Headen et al. 2014, 2018a, 2018b). Due to the slower speed of gelation for PEG-vinylsulfone, fast on-chip gelation does not impose a significant limitation. The ion-based requirements for crosslinking of alginate have synergized well with microfluidic device fabrication of alginate microgels.

One approach is to use calcium- ethylenediaminetracetic acid or calcium carbonate as the source for calcium ions, made available for crosslinking alginate by co-flowing acid-laden oil (Tan and Takeuchi 2007; Chen et al. 2016a; Zhang et al. 2018). Alternative methods involve off-chip pairing of microgels with an agarose slab containing calcium chloride. After the alginate pre-gel is sectioned into droplets within a decane and surfactant continuous phase by a flow focusing microfluidic device, the pre-microgel droplets are collected over a macro-scale agarose gel containing solubilized calcium chloride. Innate osmotic pressure differences between the agarose slab and alginate droplet drive diffusion of calcium ions into alginate microgels without the use of acids (Hirama et al. 2012). PEG-acrylate and methacrylated gelatin chemistries requiring ultraviolet light and a photo initiator have shown to be compatible with microfluidic microgel droplets (Choi et al. 2016; Lee and Cha 2018). Optically transparent microfluidic devices allow for the brief penetration of UV facilitating gelation as the droplet proceeds to be collected at the output.

3.2 Emulsification

Emulsification has been extensively studied for the preparation of hydrogel carriers due to the advantage of synthesizing hydrogels from nanometer to micrometer length scales without the specialized equipment requirements of other methods. Depending on the solubility of the desired monomers, a pre-polymer solution is chosen to form either an oil-in-water or a water-in-oil emulsion with the continuous phase upon sonication or mechanical stirring, although other systems such as water-in-water emulsions (Aydın and Kızılel 2017) have been explored. Surfactants are commonly used to improve the emulsion stability, and nonionic, cationic, anionic, zwitterionic, or a combination of surfactants can be chosen to tune the desired microdroplet size. The polymer network is then formed by either polymerization of the monomer and crosslinking agent (Yan and Gemeinhart 2005; Tokuyama and Kato 2008; González-Sánchez et al. 2011; Aydın and Kızılel 2017; Wang et al. 2018), or by physical or chemical crosslinking of the polymer (Wang et al. 2013; Morelli et al. 2016; Piacentini et al. 2017).

A wide range of homopolymer and copolymer systems have been explored with emulsion techniques including polyacrylamide (González-Sánchez et al. 2011), poly(acrylic acid) (Yan and Gemeinhart 2005), poly(ethylene glycol) (Aydın and Kızılel 2017; Wang et al. 2018), chitosan (Wang et al. 2013; Morelli et al. 2016), and poly(vinyl alcohol) (Morelli et al. 2016; Piacentini et al. 2017). For drug delivery applications, emulsion polymerization is frequently used to produce nanoparticle carriers (Sahana et al. 2008; You and Auguste 2008), which offer improved surface area-to-volume ratios; however, microparticle systems have also been studied (Yan and Gemeinhart 2005). With emulsification approaches for cell encapsulation, microparticles can be prepared by the physical or chemical crosslinking of the polymer solution to avoid cytotoxicity of many monomers and surfactants. This approach has successfully been used for the encapsulation of human mesenchymal stem cells in chitosan and collagen microbeads (Wang et al. 2013).

The major limitations of emulsification are the lack of control over particle morphology, size, and polydispersity. One strategy to produce monodisperse carriers is membrane emulsification, which forces the pre-polymer solution through a microporous membrane into an immiscible continuous phase. Membrane emulsification has been successfully used for the entrapment of lipase in poly(vinyl alcohol) (PVA) microspheres (Piacentini et al. 2017), as well as pH dependent release from chitosan and PVA microparticles (Morelli et al. 2016).

3.3 Photolithography

The use of photolithography in biomedical applications for the synthesis of microgels has grown in interest due to improved control over the size and shape of the hydrogel, in addition to greater uniformity. Photolithographic preparation of microstructures begins with coating the pre-polymer solution containing a light reactive initiator onto the surface of a wafer, which can be functionalized with reactive groups to anchor the resulting hydrogel to the surface. The pre-polymer solution is then selectively exposed to light in a desired pattern, resulting in polymerization of only the exposed regions, and then the unreacted solution is removed.

Photolithographic techniques for cell encapsulation and drug delivery have successfully used poly(ethylene glycol)

acrylates (Revzin et al. 2001; Hoffmann and West 2010), chitosan (Li et al. 2015), gelatin methacrylate (Nikkhah et al. 2012), fibrinogen (Mironi-Harpaz et al. 2015), and interpenetrating networks of collagen and hyaluronic acid (Suri and Schmidt 2009) for the creation of patterned microstructures. Compared to other synthesis methods, photolithography offers the advantage of precisely controlling particle size and shape through selective initiation without the need for the additional continuous phase required by emulsification or microfluidics for the creation of pre-patterned mold. Additionally, the ability to sequentially coat multiple layers of pre-polymer solution has been exploited to prepare multilayer microparticles of poly(N-vinyl-2-pyrrolidone) and PEG triacrylate that selectively incorporate PEG-biotin into a single layer (Li et al. 2016).

The major challenges of photolithographic microstructure synthesis come from the reliance on photo-masks for selective exposure, which are limited to two-dimensional patterns and suffer from diffraction limitations on the resolution of the resulting structures. One alternative is two photon photolithography, which can be performed by the absorption of two photons of the same wavelength (Hoffmann and West 2010), or with a combination of photoinitiator and photoinhibitor that each absorb different wavelengths (Scott et al. 2009). Because of the need to absorb two photons simultaneously, two photon photolithography offers the advantage of smaller initiation volumes, which allow for nanoscale structures in addition to three-dimensional patterns (Kawata et al. 2001; Deforest et al. 2009). For cell encapsulation, there is an additional challenge of obtaining successful crosslinking of patterned structures in the dilute pre-polymer solutions necessary for cell compatibility. In order to address this issue, microscopic laser photolithography was successfully used to pattern cell-compatible hydrogels with fibrinogen and Pluronic F127 to exploit temperature-dependent phase transitions as a way to minimize diffusion during crosslinking (Mironi-Harpaz et al. 2015).

3.4 Micromolding

Micromolding uses a patterned master template that contains a negative of the desired microstructure. The pre-polymer solution is then either filled into the mold, or pressed between the mold and a solid substrate prior to initiation, and removed once polymerization has completed, leaving structured hydrogels with the shape of the pattern's indentation. For biomedical applications, micromolding has been successfully employed for the creation of patterned microgels of natural polymers including hyaluronic acid (Khademhosseini et al. 2006), collagen (McGuigan et al. 2008), and chitosan (Fukuda et al. 2006; Jung and Yi 2015), as well as synthetic polymers including poly(ethylene-glycol) (Subramani and Birch 2009; Heath et al. 2015; Jung and Yi 2015) and poly(dimethyl siloxane) (PDMS) (Fu et al. 2010). Moreover, the Singh group previously reported a microarray of composite bioadhesive microgels, specifically, maleimide functionalized polyethylene glycol with an interpenetrating network of gelatin ionically cross-linked with silicate nanoparticles, engineered by integrating microfabrication with Michael-type addition chemistry and ionic gelation (Patel et al. 2014). These composite bioadhesive hydrogels represent a platform that could be used to study the independent effect of stiffness and adhesive ligand density on cell survival and function, as was demonstrated with select cancer cells.

Micromolding can be used to synthesize hydrogels with a variety of two-dimensional shapes, including clovers or crosses (McGuigan et al. 2008), as well three-dimensional structures, such as micropillars (Fu et al. 2010), but it is difficult to prepare patterns with a high aspect ratio or spherical structures. Recent techniques have improved the ability to generate complex microstructures. Chitosan-poly(ethylene glycol) microspheres with a core-shell structure were prepared by exploiting surface tension induced droplet formation in PDMS molds (Jung and Yi 2015). Additionally, microparticles, rather than pre-polymer solution, can be used in order to create microstructures from multiple materials (Park et al. 2007).

The ability of micromolding to simultaneously pattern multiple three-dimensional structures without the need for spin coating multiple pre-polymer layers or limiting exposure area is a significant advantage over photolithography. Despite this advantage, the need for a mold presents several challenges for micromolding approaches. For micromolding methacrylated hyperbranched polyglycerol microparticles, as many as 50% of the particles prepared using a rigid SU-8 photoresist mold were found to break apart or remain attached to the mold after the synthesis, and although switching to a flexible PDMS mold improved yield, the difficulty completely filling the mold with the pre-polymer solution led to greater defects than photolithography (Oudshoorn et al. 2007). Additionally, the use of PDMS for the patterned template has been found to increase protein adsorption and cell adhesion on PEG microstructures due to residual PDMS left behind on the surface (Heath et al. 2015).

4 Microscale hydrogels for drug delivery

Microscale hydrogels are excellent candidates for use as drug delivery carriers, especially for obtaining controlled release of therapeutic agents. The polymer carriers are primarily used for several reasons: to protect therapeutic molecules from undesired degradation, increase the efficacy of delivery, and decrease potential side effects. To obtain controlled release, the carriers help maintain the concentration of drug within the therapeutic window over an extended time, which allows for a prolonged time period between administrations (Liechty

et al. 2010; Vermonden et al. 2012). Controlled release systems are preferred compared to traditional drug delivery platforms because there is no sharp increase in drug concentration shortly following administration, preventing a potentially toxic response. In addition, the need for less frequent administration could potentially increase patient compliance.

Physical and chemical parameters of the microgels can be altered to tune their delivery properties. The structure and density of the crosslinking agent used in the formulation will affect the network mesh size, and thus the rate of the diffusion of water-soluble therapeutic drug out of the microgel (Kim and Bae 1992; Peppas et al. 2000). The diameter of the hydrogels will also affect controlled release, as a larger diameter will lead to longer release if the microgels are completely loaded with the molecule of interest. Different tissues of interest can also be targeted by altering the diameter of the microgels. For instance, microgels 1–5 μm in diameter would be best suited to passively target antigen-presenting cells (Wattendorf et al. 2008), while those 10–20 μm in diameter would be better suited to target capillary beds, especially in tumors (Salem et al. 2005).

Precision particle formation is commonly used to produce uniform particles made of various materials. This technique, which utilizes special solvent extraction and evaporation methods, has been adapted to synthesize microparticles for controlled release drug delivery platforms (Xia and Pack 2015). Precision particle formation can control the particle diameter to within one micron (Berkland et al. 2003). This work demonstrated that properties of both the drugs and the particles impact the distribution of the drug molecules within the particles, as well as the degradation and drug release rates. Furthermore, Berkland and colleagues were able to alter the particle size and shell thickness to obtain particles with zero-order, pulsatile, or tandem drug release (Berkland et al. 2003).

Moreover, the kinetics of drug release from hydrogel microcarriers can be tailored by adjusting properties of the carrier, such as monomers utilized, crosslinking density, use of a coating (to create a core-shell structure), as well as several other parameters. An example of this is the recently developed hydrogel microparticle drug delivery system comprised of poly(lactic-co-glycolic) acid (synthesized via a water-in-oil emulsion) for the release of platelet derived growth factor-AA (Pinezich et al. 2018). This specific growth factor has been studied as a signaling molecule to initiate a response in oligodendrocyte precursor cells, which can lead to proliferation or differentiation of central nervous system tissue after injury or disease. When oligodendrocyte precursor cells were exposed to drug loaded microgels, it was found that a burst release, followed by withdrawal of the growth factor, stimulated survival, proliferation, and differentiation of the cells *in vitro*. This type of system could allow the development of improved strategies for regeneration of neural tissues, which are intrinsically limited.

Understanding the conditions that affect hydrogel properties can also be used to cultivate targeted delivery strategies. For example, anionic pH-responsive materials are commonly used in oral drug delivery platforms due to their ability to protect the therapeutic molecule in the harsh gastric conditions of the stomach and then release it in the small intestine for absorption into the bloodstream (Torres-Lugo et al. 2002; Carr and Peppas 2009; Durán-Lobato et al. 2014; Koetting et al. 2016; Steichen et al. 2016; Sharpe et al. 2018). Other responsive hydrogel systems have been used in additional drug delivery platforms, such as an enzyme-responsive microgel system studied for pulmonary drug delivery (Secret et al. 2014). An inverse emulsion polymerization method was used to synthesize poly(ethylene glycol) diacrylate microparticles containing specific peptides that degrade in the presence of metalloproteinases that are overexpressed in certain pulmonary diseases such as lung cancer, tuberculosis, and chronic obstructive pulmonary disease (COPD) (Chang et al. 1996; Demedts et al. 2006; Leinonen et al. 2006; Ullah and Aatif 2009). Hydrogels are especially useful for pulmonary drug delivery because their size can be precisely engineered for bronchial delivery, but their swelling behavior prevents the microgels from uptake and clearance by macrophages in the alveoli.

5 Applications of microscale hydrogels for cell therapy

Microscale hydrogels are appealing for cell encapsulation and therapy because they are highly permeable to water and easily customizable for the cell type and application. For example, incorporation of short, cell-recognizable polypeptide sequences enhances bioactivity of the microgel, as well as allows for countless permutations of possible microgel qualities. Many PEG-based hydrogels have been developed to promote enzymatic degradation through the incorporation of protease-degradable peptides (Raeber et al. 2005; Lee et al. 2005; Phelps et al. 2012; Gould et al. 2012; Schultz and Anseth 2013). These functionalized PEG hydrogels have been used to regulate cellular responses (Cayrol et al. 2015; Lee et al. 2015), and have been engineered for the development of tissue engineering constructs (Lutolf and Hubbell 2005; Sridhar et al. 2015; Schultz et al. 2015), tumor organoids (Tian et al. 2015), and synthetic ex vivo immune tissues (Purwada et al. 2018). The diverse spectrum of cell types used for such applications each require preferred culturing conditions that can be supplied through a personalized microgel with major applications in cell therapy and *in vitro* tissue and disease models. In order to develop a microgel strategy for these uses, special considerations and validations must be implemented.

Many pre-gel chemicals, as well as the oil phase in microfluidic approaches, can threaten cell viability during

the formation and preparation of microgels. In fact, for an acid-laden oil double emulsion set-up, Zhang et al. showed that viability was best at high oil flow rates because cell contact with the oil was therefore shorter (Zhang et al. 2018). Oil cytotoxicity concerns were further addressed by introducing perfluorooctanol on-chip to destabilize oil coating on microgels and allow for fast oil removal upon collection of microgels downstream (Zhang et al. 2018). Along similar lines, a double emulsion approach minimizes the required amount of oil phase, thereby increasing viability over a single emulsion device format of aqueous gel droplets in oil (Choi et al. 2016). Microgels fabricated using the double-emulsion approach offer the added ease of spontaneous "dewetting" of oil in Dulbecco's Modified Eagle Medium (DMEM) culture media, providing for easy oil removal immediately following gelation.

Confirmation of microgel encapsulated cell viability and biological activity is critical in the validation of any microgel platform for cell therapy or *in vitro* models. Survival from the microgel fabrication process and extended culture is easily confirmed using live/dead fluorescent stains adopted by many microgel groups (Steinhilber et al. 2013; Headen et al. 2014; Chen et al. 2016a; Choi et al. 2016; Zhang et al. 2018). Following proof of cell survival in microgels, biological activity and proliferation of cells should be assessed. This second step is arguably more important because it determines the biological relevance of the biomaterial and microgel parameters. For example, in encapsulating pancreatic islet cells for targeted cell delivery, insulin secretion should remain undisrupted by the surrounding microgel (Headen et al. 2014).

By adopting non-cytotoxic crosslinking chemistries, cell viability is easily sustained through microgel fabrication and beyond. One main driver for this approach is the development of modular, high-throughput three-dimensional cell culture models. Siltanen and colleagues demonstrated the efficacy of heparin-PEG microgels dosed with the growth factors Nodal and FGF-2 in directing the differentiation of mouse embryonic stem cells toward an endoderm lineage (Siltanen et al. 2016). This approach showed differentiation potential similar to hanging droplet cultures but at a far higher throughput by fabricating hydrogel droplets in a microfluidic device. Other cell microgel culture models include a bilayered alginate model of the liver by encapsulating hepatocytes surrounded by fibroblasts in the outer alginate layer (Chen et al. 2016b). Three-dimensional cancer models are also increasingly desired as platforms for drug discovery and dose finding. In a tumor model of prostate cancer, hyaluronic acid microgel models drove overexpression of two multi-drug resistant genes greater than two-dimensional culture (Xu et al. 2011). Additionally, there are models devoted to development of a mesenchymal stem cell niche (Lienemann et al. 2017), some with applications for immunoprotected cell therapy (Headen et al. 2018a). While there have been several microgel approaches proposed for cell therapeutic delivery, many simply propose this application, and stop short of validating utility using *in vivo* studies.

Microgel delivery of cells has been a promising solution to immune rejection of donor cells (Headen et al. 2014) which causes cell death and limits the therapeutic window of cell therapy. Immunoisolation of cells using microgels is achieved in two ways: most commonly, by physical isolation from immune cells by the biomaterial (Headen et al. 2014; Mao et al. 2017; Bochenek et al. 2018), but also by inducing localized immune suppression through apoptosis of adaptive immune cells (Headen et al. 2018b). The latter approach utilized T cell sensitivity to Fas ligand (Fas-L) following activation. By presenting biotin-streptavidin conjugated Fas-L to microgel surfaces, immune response to co-delivered unmodified donor islet cells was diminished through depletion of effector T cells while regulatory T cells remain (Fig. 4a). This approach is notable because it demonstrates the use of microgels as drivers of immune tolerance for cell therapy when the physical encapsulation of cells in microgels is not required.

Since the inception of microgel technology, it has been proposed as possible platform for cell-based insulin delivery for a long-term solution to insulin-resistant diabetes (Lim and Sun 1980). In line with disappointing clinical trials for islet encapsulated alginate microgels, recent work in the hydrogel-mediated cell delivery field may suggest that gels larger than the microscale are a better conduit than microgels for promoting immune tolerance to encapsulated cell therapy. Comparison of the fibrotic response to alginate gels in mouse peritoneum showed that hydrogel spheres up to 1.9 mm in diameter demonstrated markedly less cellular deposition of macrophages and myofibroblasts compared to microscale gels (Veiseh et al. 2015). Size-dependent foreign body response was conserved in several of the other biomaterials compared (Veiseh et al. 2015). This size theory was later confirmed in non-human primates, when delivery of allogeneic pancreatic islet cells survived 4 months of implantation in modified alginate spheres 1.5 mm in size and further exhibited minimal signs of a foreign-body response (Bochenek et al. 2018) (Fig. 4b). This study highlighted the importance of hydrogel placement, alginate chemistry, and gel size on the foreign body response, and provided strong evidence for the validity of cell encapsulation in hydrogel beads as an effective method of immunoisolation for long-term cell therapy.

Alternatively, it should be considered that encapsulated cells for cell therapy may not require long-term survival or microgel maintenance in every application. In an ischemic model, arginine-glycine-aspartic acid (RGD)-modified alginate microgels were used to deliver human outgrowth endothelial cells and blood vessel sprouting growth factors VEGF and HGF in mice (Kim et al. 2014). In this study, long-term cell viability and microgel biocompatibility was not confirmed, but rather the appearance of new blood vessel in a

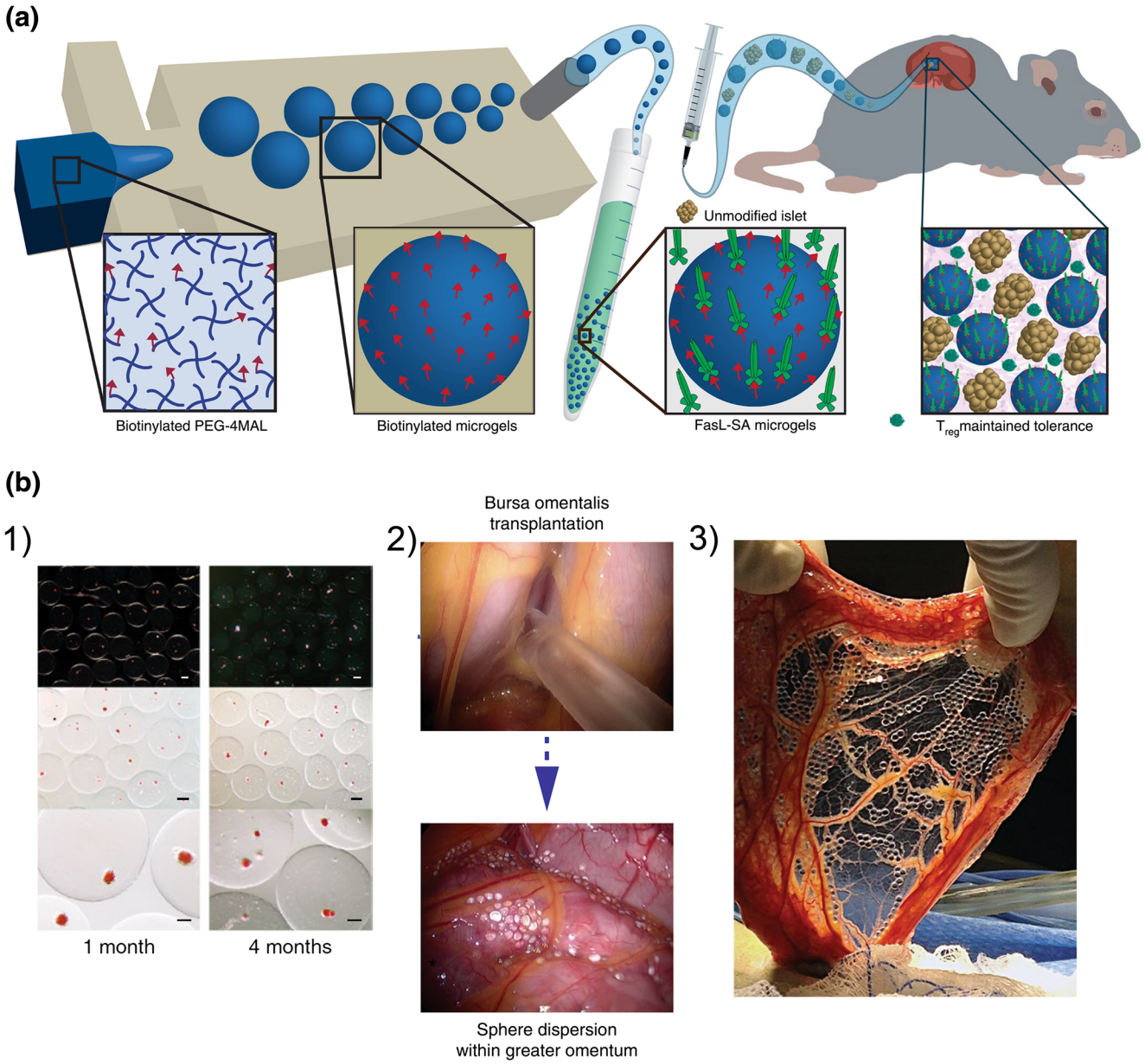

Fig. 4 **a** Fabrication process of immune modulating microgels with biotin-streptavidin surface modification to present Fas ligand. These microgels drive effector T cell apoptosis while maintaining immune-tolerant regulatory T cells in a cell therapy implantation site to sustain insulin delivery from donor islet cells. Reprinted by permission from Springer Nature: Springer, Nature Materials (Headen et al. 2018b), Copyright (2018). **b** Explanted and implanted allogeneic pancreatic islet cells in modified alginate spheres. 1) Explanted modified alginate Z1-Y15 beads with encapsulated islet cells after 1 month and 4 months in a non-human primate. Cells were stained with dithizone (red) to demonstrate sustained insulin production 2) Gels showed minimal clumping in experimental implantation site, the bursa omentalis in the abdomen. 3) Explanted gels nested within the greater omentum remained visibly clear and loosely lodged in connective tissue, demonstrating minimal immune response to donor cells and modified alginate gels. Figure adapted and reprinted by permission from Springer Nature: Springer, Nature Biomedical Engineering (Bochenek et al. 2018), Copyright (2018)

mouse hindlimb ischemia model proved its success as a cell therapy approach. This application provides an alternate look at cell therapy in microgels and widens their application to more than just the long-term, cell-based production of bioproducts.

Additionally, microgel approaches to tissue engineering and cell therapy have looked at how microgel-formed macropores mitigate immune response to biomaterial implantation. The latter was achieved by engineering a microgel system with dual crosslinking mechanisms whereby initial microgel formation occurs on chip, and secondary microgel crosslinking establishes connections between microgels (Griffin et al. 2015). Cells can be incorporated during secondary crosslinking to form a cell-laden hydrogel with macropores. This two-pronged approached was also evaluated for use in a wound healing model without the addition of cells and found that the presence of these pores increased immune cell penetration into the material rather than

accumulating at the surface and initiating the foreign body response. Evidence of reduced immune response was maintained out to 5 days post-implantation. This approach provides the framework for an additional microgel application where implanted cells or infiltrating cells from the wound healing process inhabit the negative space surrounding microgels rather than from within microgels. Additionally, this promising achievement successfully bridges advances in microgel technology with macro-scale biomaterials applications and expands the microgel application realm from drug delivery and cell therapy to tissue engineering and regenerative medicine.

6 Future outlook

Independent of the progress of biomedical microgel research, the scientific community has entered into "the genomic era" (Guttmacher and Collins 2003) as the cost of sequencing genomes, transcriptomes, proteomes, and the ever expanding other "omes" has diminished as the technologies have improved. Many of the recent advances in the sequencing field involve scaling size down to the single-cell sampling level. This approach is necessary because sequencing in bulk samples produces information on the population level, losing key information about biological subsets within the sample (Trapnell 2015). By partitioning single cells into separate wells or droplets, individualized sequencing can be performed producing 'omic' data on a cell by cell level. In this way, outlier populations are not buried by the population average and sample heterogeneity is brought to light. Single-cell sequencing, similar to microgel fabrication, has benefited from microfluidic water-in-oil emulsions to separate cells into individual droplets that serve as personalized cell bioreactors for nucleic acid barcoding and other pre-sequencing steps. This approach has successfully allowed for high-throughput single-cell sequencing of DNA (Lan et al. 2017; Demaree et al. 2018), mRNA (Klein et al. 2015; Macosko et al. 2015; Zilionis et al. 2017), chromatin states (CHIP-seq) (Wu et al. 2009; Rotem et al. 2015; Murphy et al. 2018), immune repertoires (Vollmers et al. 2013), and multiplexed mRNA and protein expression (Stoeckius et al. 2017).

Simultaneously, microgels and microbeads are permeating the sequencing sphere. Many sequencing schemes are based off of the technique Dropseq (Macosko et al. 2015), combining single cells with oligonucleotide barcodes extending from a hydrogel bead. These beads work by collecting nucleic acids and serve as an easy method for transcript barcoding. Each bead contains oligonucleotide barcode sequences that are unique to the bead, and incorporation of this barcode into the collected material tags it by each source cell. Bead pairing on a chip is used in Dropseq and InDrops single cell mRNA sequencing (Klein et al. 2015; Macosko et al. 2015; Zilionis et al. 2017), CITE-seq mRNA sequencing paired with epitope expression (Stoeckius et al. 2017), single cell ChIP-seq (Rotem et al. 2015) and LIFE-ChIP-seq (Murphy et al. 2018) chromatin mapping, DroNc-seq intranuclear RNA sequencing (Murphy et al. 2018), and SiC-seq single cell genome sequencing(Lan et al. 2017). In addition to microgels, immobile hydrogels are synergizing with digital microfluidic devices as microscale bioreactors (Fiddes et al. 2012). Luk et al. proposed combining digital microfluidics with agarose gels as microscale liquid handling system for multiplexing enzyme digestion of protein samples for proteomic studies (Luk et al. 2012). In this work, solid agarose discs were chemically modified and conjugated to the enzymes of interest, thereby fixing them in space, simplifying the task of sample and enzyme after digestion.

These examples demonstrate the early stages of the convergence of microgels and sequencing technology development. The authors envision this marriage to continue to develop as the symbiotic utility of these fields is further explored. For example, oiligonucleotide barcoded beads could be combined with cell-laden microgels on-chip to track cell-fate and population heterogeneity following challenge with time, growth factors, environmental stimuli, and drug exposure. Such a model would provide clues to developmental biology, infectious disease, cancer research and the heterogeneity of cell therapy.

Acknowledgements This work is submitted in honor of Professor Mauro Ferrari's 60th birthday. Mauro has been an inspirational force in the fields of nanotechnology and bionanotechnology. His writings have been extremely important in defining these fields, and the senior authors who have known him and worked with him appreciate all the contributions he has made to their research, directly and indirectly.

We acknowledge financial support from the National Institutes of Health (R01-AI132738-01A1 and 5R33CA212968-02 awarded to AS; R01-EB022025 awarded to NAP), the National Science Foundation CAREER award (DMR-1554275 awarded to AS), Department of Defense CDMRP and Cancer Career Development Award (W81XWH-17-1-0215 awarded to AS). In addition, NAP acknowledges support from the Cockrell Family Chair Foundation and the office of the Dean of the Cockrell School of Engineering at the University of Texas at Austin for the Institute for Biomaterials, Drug Delivery, and Regenerative Medicine. We acknowledge financial support from the National Science Foundation Graduate Research Fellowship Program (DGE-1610403 awarded to MEW; DGE-1650441 awarded to RES). Any opinions, findings, and conclusions or recommendations expressed in this material are those of the author(s) and do not necessarily reflect the views of the funding agencies.

References

S. Allazetta, T.C. Hausherr, M.P. Lutolf, Microfluidic synthesis of cell-type-specific artificial extracellular matrix hydrogels. Biomacromolecules **14**, 1122–1131 (2013). https://doi.org/10.1021/bm4000162

D. Aydın, S. Kızılel, Water-in-water emulsion based synthesis of hydrogel Nanospheres with tunable release kinetics. JOM **69**, 1185 (2017). https://doi.org/10.1007/s11837-016-1969-z

C. Berkland, K. Kim, D.W. Pack, PLG Microsphere Size Controls Drug Release Rate Through Several Competing Factors. Pharm. Res. **20**, 1055–1062 (2003). https://doi.org/10.1023/A:1024466407849

M.A. Bochenek, O. Veiseh, A.J. Vegas, et al., Alginate encapsulation as long-term immune protection of allogeneic pancreatic islet cells transplanted into the omental bursa of macaques. Nat Biomed Eng **2**, 810 (2018)

L. Brannon-Peppas, N.A. Peppas, Dynamic and equilibrium swelling behaviour of pH-sensitive hydrogels containing 2-hydroxyethyl methacrylate. Biomaterials **11**, 635–644 (1990)

M. Caldorera-Moore, M.K. Kang, Z. Moore, et al., Swelling behavior of nanoscale, shape- and size-specific, hydrogel particles fabricated using imprint lithography. Soft Matter **7**, 2879 (2011). https://doi.org/10.1039/c0sm01185a

D.A. Carr, N.A. Peppas, Assessment of poly(methacrylic acid- *co* - *N* -vinyl pyrrolidone) as a carrier for the oral delivery of therapeutic proteins using Caco-2 and HT29-MTX cell lines. J. Biomed. Mater. Res. Part A 9999A, NA-NA (2009). https://doi.org/10.1002/jbm.a.32395

F. Cayrol, M.C. Diaz Flaque, T. Fernando, et al., Integrin v 3 acting as membrane receptor for thyroid hormones mediates angiogenesis in malignant T cells. Blood **125**, 841–851 (2015). https://doi.org/10.1182/blood-2014-07-587337

J.C. Chang, A. Wysocki, K.M. Tchou-Wong, et al., Effect of Mycobacterium tuberculosis and its components on macrophages and the release of matrix metalloproteinases. Thorax **51**, 306–311 (1996)

Q. Chen, D. Chen, J. Wu, J.M. Lin, Flexible control of cellular encapsulation, permeability, and release in a droplet-templated bifunctional copolymer scaffold. Biomicrofluidics **10**, 1–9 (2016a). https://doi.org/10.1063/1.4972107

Q. Chen, S. Utech, D. Chen, et al., Controlled assembly of heterotypic cells in a core-shell scaffold: Organ in a droplet. Lab Chip **16**, 1346 (2016b). https://doi.org/10.1039/c6lc00231e

C.-H. Choi, H. Wang, H. Lee, et al., One-step generation of cell-laden microgels using double emulsion drops with a sacrificial ultra-thin oil shell. Lab Chip **16**, 1549–1555 (2016). https://doi.org/10.1039/C6LC00261G

J. Crank, *The Mathematics of Diffusion*, 2nd edn. (Oxford University Press, New York, 1975)

H.R. Culver, N.A. Peppas, Protein-imprinted polymers: The shape of things to come? Chem. Mater. **29**, 5753–5761 (2017). https://doi.org/10.1021/acs.chemmater.7b01936

C.A. Deforest, B.D. Polizzotti, K.S. Anseth, Sequential click reactions for synthesizing and patterning three-dimensional cell microenvironments. Nat. Mater. **8**, 659 (2009). https://doi.org/10.1038/nmat2473

B. Demaree, D. Weisgerber, F. Lan, A.R. Abate, An ultrahigh-throughput microfluidic platform for single-cell genome sequencing. J. Vis. Exp. **57598** (2018). https://doi.org/10.3791/57598

I.K. Demedts, A. Morel-Montero, S. Lebecque, et al., Elevated MMP-12 protein levels in induced sputum from patients with COPD. Thorax **61**, 196–201 (2006). https://doi.org/10.1136/thx.2005.042432

M. Durán-Lobato, B. Carrillo-Conde, Y. Khairandish, N.A. Peppas, Surface-modified P(HEMA- *co* -MAA) Nanogel carriers for Oral vaccine delivery: Design, characterization, and *in vitro* targeting evaluation. Biomacromolecules **15**, 2725–2734 (2014). https://doi.org/10.1021/bm500588x

L.K. Fiddes, V.N. Luk, S.H. Au, et al., Hydrogel discs for digital microfluidics. Biomicrofluidics **6**, 14112 (2012). https://doi.org/10.1063/1.3687381

P.J. Flory, J. Rehner, Statistical mechanics of cross-linked polymer networks I. rubberlike elasticity. J. Chem. Phys. **11**, 512–520 (1943). https://doi.org/10.1063/1.1723791

G.A. Foster, D.M. Headen, C. González-García, et al., Protease-degradable microgels for protein delivery for vascularization. Biomaterials **113**, 170–175 (2017). https://doi.org/10.1016/j.biomaterials.2016.10.044

J. Fu, Y.K. Wang, M.T. Yang, et al., Mechanical regulation of cell function with geometrically modulated elastomeric substrates. Nat. Methods **7**, 733 (2010). https://doi.org/10.1038/nmeth.1487

J. Fukuda, A. Khademhosseini, Y. Yeo, et al., Micromolding of photocrosslinkable chitosan hydrogel for spheroid microarray and co-cultures. Biomaterials **27**, 5259 (2006). https://doi.org/10.1016/j.biomaterials.2006.05.044

M.I. González-Sánchez, J. Rubio-Retama, E. López-Cabarcos, E. Valero, Development of an acetaminophen amperometric biosensor based on peroxidase entrapped in polyacrylamide microgels. Biosens. Bioelectron. **26**, 1883 (2011). https://doi.org/10.1016/j.bios.2010.03.024

S.T. Gould, N.J. Darling, K.S. Anseth, Small peptide functionalized thiol–ene hydrogels as culture substrates for understanding valvular interstitial cell activation and *de novo* tissue deposition. Acta Biomater. **8**, 3201–3209 (2012). https://doi.org/10.1016/j.actbio.2012.05.009

S.E.A. Gratton, P.D. Pohlhaus, J. Lee, et al., Nanofabricated particles for engineered drug therapies: A preliminary biodistribution study of PRINT™ nanoparticles. J. Control. Release **121**, 10 (2007). https://doi.org/10.1016/j.jconrel.2007.05.027

D.R. Griffin, W.M. Weaver, P.O. Scumpia, et al., Accelerated wound healing by injectable microporous gel scaffolds assembled from annealed building blocks. Nat. Mater. **14**, 737–744 (2015). https://doi.org/10.1038/nmat4294

A.E. Guttmacher, F.S. Collins, Welcome to the genomic era. N. Engl. J. Med. **349**, 996 (2003). https://doi.org/10.1056/NEJMe038132

D.M. Headen, G. Aubry, H. Lu, A.J. García, Microfluidic-based generation of size-controlled, biofunctionalized synthetic polymer microgels for cell encapsulation. Adv. Mater. **26**, 3003–3008 (2014). https://doi.org/10.1002/adma.201304880

D.M. Headen, J.R. García, A.J. García, Parallel droplet microfluidics for high throughput cell encapsulation and synthetic microgel generation. Microsyst. Nanoeng. **4**, 17076 (2018a). https://doi.org/10.1038/micronano.2017.76

D.M. Headen, K.B. Woodward, M.M. Coronel, et al., Local immunomodulation with Fas ligand-engineered biomaterials achieves allogeneic islet graft acceptance. Nat. Mater. **17**, 732–739 (2018b). https://doi.org/10.1038/s41563-018-0099-0

D.E. Heath, A.R.M. Sharif, C.P. Ng, et al., Regenerating the cell resistance of micromolded PEG hydrogels. Lab Chip **15**, 2073 (2015). https://doi.org/10.1039/c4lc01416b

H. Hirama, T. Kambe, K. Aketagawa, et al., Hyper alginate gel microbead formation by molecular diffusion at the hydrogel/droplet Interface. Langmuir **29**, 519–524 (2012). https://doi.org/10.1021/la303827u

J.C. Hoffmann, J.L. West, Three-dimensional photolithographic patterning of multiple bioactive ligands in poly(ethylene glycol) hydrogels. Soft Matter **6**, 5056 (2010). https://doi.org/10.1039/c0sm00140f

S. Jung, H. Yi, Facile micromolding-based fabrication of biopolymeric - synthetic hydrogel microspheres with controlled structures for improved protein conjugation. Chem. Mater. **27**, 3988 (2015). https://doi.org/10.1021/acs.chemmater.5b00920

S. Kawata, H.-B. Sun, T. Tanaka, K. Takada, Finer features for functional microdevices. Nature **412**, 697–698 (2001). https://doi.org/10.1038/35089130

A. Khademhosseini, G. Eng, J. Yeh, et al., Micromolding of photocrosslinkable hyaluronic acid for cell encapsulation and entrapment. J. Biomed. Mater. Res. Part A. **79A**, 522 (2006). https://doi.org/10.1002/jbm.a.30821

S.W. Kim, Y.H.O.T. Bae, Hydrogels: swelling, drug loading, and release. Pharm. Res. **9**, 283–290 (1992)

P.-H. Kim, H.-G. Yim, Y.-J. Choi, et al., Injectable multifunctional microgel encapsulating outgrowth endothelial cells and growth factors for enhanced neovascularization. J. Control. Release **187**, 1–13 (2014). https://doi.org/10.1016/j.jconrel.2014.05.010

A.M. Klein, D.A. Weitz, M.W. Kirschner, et al., Droplet barcoding for single-cell transcriptomics applied to embryonic stem cells. Cell **161**, 1187–1201 (2015). https://doi.org/10.1016/j.cell.2015.04.044

M.C. Koetting, J.F. Guido, M. Gupta, et al., pH-responsive and enzymatically-responsive hydrogel microparticles for the oral delivery of therapeutic proteins: Effects of protein size, crosslinking density, and hydrogel degradation on protein delivery. J. Control. Release **221**, 18–25 (2016). https://doi.org/10.1016/j.jconrel.2015.11.023

R.W. Korsmeyer, R. Gurny, E. Doelker, et al., Mechanisms of solute release from porous hydrophilic polymers. Int. J. Pharm. **15**, 25–35 (1983). https://doi.org/10.1016/0378-5173(83)90064-9

F. Lan, B. Demaree, N. Ahmed, A.R. Abate, Single-cell genome sequencing at ultra-high-throughput with microfluidic droplet barcoding. Nat. Biotechnol. **35**, 640–646 (2017). https://doi.org/10.1038/nbt.3880

D. Lee, C. Cha, Combined effects of co-culture and substrate mechanics on 3D tumor spheroid formation within microgels prepared via flow-focusing microfluidic fabrication. Pharmaceutics **10**, 1–14 (2018). https://doi.org/10.3390/pharmaceutics10040229

S.-H. Lee, J.S. Miller, J.J. Moon, J.L. West, Proteolytically degradable hydrogels with a Fluorogenic substrate for studies of cellular proteolytic activity and migration. Biotechnol. Prog. **21**, 1736–1741 (2005). https://doi.org/10.1021/bp0502429

T.T. Lee, J.R. García, J.I. Paez, et al., Light-triggered *in vivo* activation of adhesive peptides regulates cell adhesion, inflammation and vascularization of biomaterials. Nat. Mater. **14**, 352–360 (2015). https://doi.org/10.1038/nmat4157

T. Leinonen, R. Pirinen, J. Böhm, et al., Expression of matrix metalloproteinases 7 and 9 in non-small cell lung cancer: Relation to clinicopathological factors, β-catenin and prognosis. Lung Cancer **51**, 313–321 (2006). https://doi.org/10.1016/J.LUNGCAN.2005.11.002

B. Li, L. Wang, F. Xu, et al., Hydrosoluble, UV-crosslinkable and injectable chitosan for patterned cell-laden microgel and rapid transdermal curing hydrogel *in vivo*. Acta Biomater. **22**, 59 (2015). https://doi.org/10.1016/j.actbio.2015.04.026

B. Li, M. He, L. Ramirez, et al., Multifunctional hydrogel microparticles by polymer-assisted photolithography. ACS Appl. Mater. Interfaces **8**, 4158 (2016). https://doi.org/10.1021/acsami.5b11883

W.B. Liechty, D.R. Kryscio, B.V. Slaughter, N.A. Peppas, Polymers for drug delivery systems. Annu. Rev. Chem. Biomol. Eng. **1**, 149–173 (2010). https://doi.org/10.1146/annurev-chembioeng-073009-100847

P.S. Lienemann, T. Rossow, A.S. Mao, et al., Single cell-laden protease-sensitive microniches for long-term culture in 3D. Lab Chip **17**, 727–737 (2017). https://doi.org/10.1039/C6LC01444E

F. Lim, A.M. Sun, Microencapsulated islets as bioartificial endocrine pancreas. Science **210**, 908–910 (1980)

A.M. Lowman, T.D. Dziubla, P. Bures, N.A. Peppas, Structural and dynamic response of neutral and intelligent networks in biomedical environments. Adv. Chem. Eng. **29**, 75–130 (2004). https://doi.org/10.1016/S0065-2377(03)29004-9

V.N. Luk, L.K. Fiddes, V.M. Luk, et al., Digital microfluidic hydrogel microreactors for proteomics. Proteomics **12**, 1310–1318 (2012). https://doi.org/10.1002/pmic.201100608

M.P. Lutolf, J.A. Hubbell, Synthetic biomaterials as instructive extracellular microenvironments for morphogenesis in tissue engineering. Nat. Biotechnol. **23**, 47–55 (2005). https://doi.org/10.1038/nbt1055

E.Z. Macosko, A. Basu, A. Regev, et al., Highly parallel genome-wide expression profiling of individual cells using Nanoliter droplets Resource Highly Parallel Genome-wide Expression Profiling of Individual Cells Using Nanoliter Droplets. Cell **161**, 1202–1214 (2015). https://doi.org/10.1016/j.cell.2015.05.002

A.S. Mao, J.-W. Shin, S. Utech, et al., Deterministic encapsulation of single cells in thin tunable microgels for niche modelling and therapeutic delivery. Nat. Mater. **16**, 236–243 (2017). https://doi.org/10.1038/nmat4781

A.P. McGuigan, D.A. Bruzewicz, A. Glavan, et al., Cell encapsulation in sub-mm sized gel modules using replica molding. PLoS One **3**, e2258 (2008). https://doi.org/10.1371/journal.pone.0002258

I. Mironi-Harpaz, L. Hazanov, G. Engel, et al., In-situ architectures designed in 3D cell-laden hydrogels using microscopic laser photolithography. Adv. Mater. **27**, 1933 (2015). https://doi.org/10.1002/adma.201404185

S. Morelli, R.G. Holdich, M.M. Dragosavac, Chitosan and poly (vinyl alcohol) microparticles produced by membrane emulsification for encapsulation and pH controlled release. Chem. Eng. J. **288**, 451 (2016). https://doi.org/10.1016/j.cej.2015.12.024

T.W. Murphy, Y.-P. Hsieh, S.S. Ma, et al., Microfluidic low-input fluidized-bed enabled ChIP-seq device for automated and parallel analysis of histone modifications. Anal. Chem. **90**, 7666–7674 (2018). https://doi.org/10.1021/acs.analchem.8b01541

M.I. Neves, M.E. Wechsler, M.E. Gomes, et al., Molecularly imprinted intelligent scaffolds for tissue engineering applications. Tissue Eng. B Rev. **23**, 27–43 (2017). https://doi.org/10.1089/ten.TEB.2016.0202

M. Nikkhah, N. Eshak, P. Zorlutuna, et al., Directed endothelial cell morphogenesis in micropatterned gelatin methacrylate hydrogels. Biomaterials **33**, 9009 (2012). https://doi.org/10.1016/j.biomaterials.2012.08.068

M.H.M. Oudshoorn, R. Penterman, R. Rissmann, et al., Preparation and characterization of structured hydrogel microparticles based on cross-linked hyperbranched polyglycerol. Langmuir **23**, 11819 (2007). https://doi.org/10.1021/la701910d

J.H. Park, S.O. Choi, R. Kamath, et al., Polymer particle-based micromolding to fabricate novel microstructures. Biomed. Microdevices **9**, 223 (2007). https://doi.org/10.1007/s10544-006-9024-4

R.G. Patel, A. Purwada, L. Cerchietti, et al., Microscale bioadhesive hydrogel arrays for cell engineering applications. Cell. Mol. Bioeng. **7**, 394 (2014). https://doi.org/10.1007/s12195-014-0353-8

N.A. Peppas, *Hydrogels in Medicine and Pharmacy* (CRC Press, Boca Raton, 1986)

N.A. Peppas, E.W. Merrill, Crosslinked poly(vinyl alcohol) hydrogels as swollen elastic networks. J. Appl. Polym. Sci. **21**, 1763–1770 (1977). https://doi.org/10.1002/app.1977.070210704

N.A. Peppas, B. Narasimhan, Mathematical models in drug delivery: How modeling has shaped the way we design new drug delivery systems. J. Control. Release **190**, 75–81 (2014). https://doi.org/10.1016/j.jconrel.2014.06.041

N.A. Peppas, P. Bures, W. Leobandung, H. Ichikawa, Hydrogels in pharmaceutical formulations. Eur. J. Pharm. Biopharm. **50**, 27–46 (2000). https://doi.org/10.1016/S0939-6411(00)00090-4

N.A. Peppas, J.Z. Hilt, A. Khademhosseini, R. Langer, Hydrogels in biology and medicine: From molecular principles to bionanotechnology. Adv. Mater. **18**, 1345–1360 (2006). https://doi.org/10.1002/adma.200501612

E.A. Phelps, N.O. Enemchukwu, V.F. Fiore, et al., Maleimide cross-linked bioactive PEG hydrogel exhibits improved reaction kinetics and cross-linking for cell encapsulation and *in situ* delivery. Adv. Mater. **24**(64–70), 2 (2012). https://doi.org/10.1002/adma.201103574

E. Piacentini, M. Yan, L. Giorno, Development of enzyme-loaded PVA microspheres by membrane emulsification. J. Membr. Sci. **524**, 79 (2017). https://doi.org/10.1016/j.memsci.2016.11.008

M.R. Pinezich, L.N. Russell, N.P. Murphy, K.J. Lampe, Encapsulated oligodendrocyte precursor cell fate is dependent on PDGF-AA release kinetics in a 3D microparticle-hydrogel drug delivery system. J. Biomed. Mater. Res. A **106**, 2402–2411 (2018). https://doi.org/10.1002/jbm.a.36432

A. Purwada, S.B. Shah, W. Béguelin, et al., Ex vivo synthetic immune tissues with T cell signals for differentiating antigen-specific, high affinity germinal center B cells. Biomaterials (2018). https://doi.org/10.1016/j.biomaterials.2018.06.034

G.P. Raeber, M.P. Lutolf, J.A. Hubbell, Molecularly engineered PEG hydrogels: A novel model system for Proteolytically mediated cell migration. Biophys. J. **89**, 1374–1388 (2005). https://doi.org/10.1529/biophysj.104.050682

A. Revzin, R.J. Russell, V.K. Yadavalli, et al., Fabrication of poly(ethylene glycol) hydrogel microstructures using photolithography. Langmuir **17**, 5440 (2001). https://doi.org/10.1021/la010075w

T. Rossow, J.A. Heyman, A.J. Ehrlicher, et al., Controlled synthesis of cell-laden microgels by radical-free gelation in droplet microfluidics. J. Am. Chem. Soc. (2012). https://doi.org/10.1021/ja300460p

A. Rotem, O. Ram, N. Shoresh, et al., Single-cell ChIP-seq reveals cell subpopulations defined by chromatin state HHS public access author manuscript. Nat. Biotechnol. **33**, 1165–1172 (2015). https://doi.org/10.1038/nbt.3383

D.K. Sahana, G. Mittal, V. Bhardwaj, M.N.V.R. Kumar, PLGA nanoparticles for oral delivery of hydrophobic drugs: Influence of organic solvent on nanoparticle formation and release behavior *in vitro* and *in vivo* using estradiol as a model drug. J. Pharm. Sci. **97**, 1530 (2008). https://doi.org/10.1002/jps.21158

R. Salem, R.J. Lewandowski, B. Atassi, et al., Treatment of Unresectable hepatocellular carcinoma with use of 90Y microspheres (TheraSphere): Safety, tumor response, and survival. J. Vasc. Interv. Radiol. **16**, 1627–1639 (2005). https://doi.org/10.1097/01.RVI.0000184594.01661.81

K.M. Schultz, K.S. Anseth, Monitoring degradation of matrix metalloproteinases-cleavable PEG hydrogels via multiple particle tracking microrheology. Soft Matter **9**, 1570–1579 (2013). https://doi.org/10.1039/C2SM27303A

K.M. Schultz, K.A. Kyburz, K.S. Anseth, Measuring dynamic cell–material interactions and remodeling during 3D human mesenchymal stem cell migration in hydrogels. Proc. Natl. Acad. Sci. **112**, E3757–E3764 (2015). https://doi.org/10.1073/pnas.1511304112

T.F. Scott, B.A. Kowalski, A.C. Sullivan, et al., Two-color single photon Photoinitiation and Photoinhibition for subdiffraction photolithography. Science **324**, 913–917 (2009). https://doi.org/10.1126/science.116761

E. Secret, S.J. Kelly, K.E. Crannell, J.S. Andrew, Enzyme-responsive hydrogel microparticles for pulmonary drug delivery. ACS Appl. Mater. Interfaces **6**, 10313–10321 (2014). https://doi.org/10.1021/am501754s

L.A. Sharpe, J.E. Vela Ramirez, O.M. Haddadin, et al., pH-responsive microencapsulation Systems for the Oral Delivery of Polyanhydride nanoparticles. Biomacromolecules **19**, 793–802 (2018). https://doi.org/10.1021/acs.biomac.7b01590

C. Siltanen, M. Yaghoobi, A. Haque, et al., Microfluidic fabrication of bioactive microgels for rapid formation and enhanced differentiation of stem cell spheroids. Acta Biomater. **34**, 125–132 (2016). https://doi.org/10.1016/J.ACTBIO.2016.01.012

B.V. Slaughter, S.S. Khurshid, O.Z. Fisher, et al., Hydrogels in regenerative medicine. Adv. Mater. **21**, 3307–3329 (2009). https://doi.org/10.1002/adma.200802106

B.V. Sridhar, J.L. Brock, J.S. Silver, et al., Development of a cellularly degradable PEG hydrogel to promote articular cartilage extracellular matrix deposition. Adv. Healthc. Mater. **4**, 702–713 (2015). https://doi.org/10.1002/adhm.201400695

S. Steichen, C. O'Connor, N.A. Peppas, Development of a P((MAA-co-NVP)-g-EG) hydrogel platform for Oral protein delivery: Effects of hydrogel composition on environmental response and protein partitioning. Macromol. Biosci. **17**, 1600266 (2016). https://doi.org/10.1002/mabi.201600266

D. Steinhilber, T. Rossow, S. Wedepohl, et al., Angewandte Chemie stimuli-responsive microgels a microgel construction kit for bioorthogonal encapsulation and pH-controlled release of living cells. Angew. Chem. Int. Ed. **52**, 13538 (2013). https://doi.org/10.1002/anie.201308005

M. Stoeckius, C. Hafemeister, W. Stephenson, et al., Simultaneous epitope and transcriptome measurement in single cells. Nat. Methods **14**, 865–868 (2017). https://doi.org/10.1038/nmeth.4380

K. Subramani, M.A. Birch, Micropatterning of Poly (Ethylene Glycol)-Diacrylate (PEG-DA) Hydrogel by Soft-Photolithography for Analysis of Cell-Biomaterial interactions. J. Biomimetics Biomater. Tissue Eng. (2009). https://doi.org/10.4028/www.scientific.net/JBBTE.2.3

S. Suri, C.E. Schmidt, Photopatterned collagen-hyaluronic acid interpenetrating polymer network hydrogels. Acta Biomater. **5**, 2385 (2009). https://doi.org/10.1016/j.actbio.2009.05.004

W.-H. Tan, S. Takeuchi, Monodisperse alginate hydrogel microbeads for cell encapsulation. Adv. Mater. **19**, 2696–2701 (2007). https://doi.org/10.1002/adma.200700433

Y.F. Tian, H. Ahn, R.S. Schneider, et al., Integrin-specific hydrogels as adaptable tumor organoids for malignant B and T cells. Biomaterials **73**, 110–119 (2015). https://doi.org/10.1016/j.biomaterials.2015.09.007

H. Tokuyama, Y. Kato, Preparation of poly(N-isopropylacrylamide) emulsion gels and their drug release behaviors. Colloids Surf. B: Biointerfaces **67**, 92 (2008). https://doi.org/10.1016/j.colsurfb.2008.08.003

M. Torres-Lugo, M. García, R. Record, N.A. Peppas, Physicochemical behavior and cytotoxic effects of p(methacrylic acid–g-ethylene glycol) nanospheres for oral delivery of proteins. J. Control. Release **80**, 197–205 (2002). https://doi.org/10.1016/S0168-3659(02)00027-5

C. Trapnell, Defining cell types and states with single-cell genomics. Genome Res. **25**, 1491 (2015)

M.F. Ullah, M. Aatif, The footprints of cancer development: Cancer biomarkers. Cancer Treat. Rev. **35**, 193–200 (2009). https://doi.org/10.1016/J.CTRV.2008.10.004

O. Veiseh, J.C. Doloff, M. Ma, et al., Size- and shape-dependent foreign body immune response to materials implanted in rodents and non-human primates. Nat. Mater. **14**, 643–651 (2015). https://doi.org/10.1038/nmat4290

T. Vermonden, R. Censi, W.E. Hennink, Hydrogels for Protein Delivery. Chem. Rev. **112**, 2853–2888 (2012). https://doi.org/10.1021/cr200157d

C. Vollmers, R.V. Sit, J.A. Weinstein, et al., Genetic measurement of memory B-cell recall using antibody repertoire sequencing. Proc. Natl. Acad. Sci. **110**, 13463 (2013). https://doi.org/10.1073/pnas.1312146110

L. Wang, R.R. Rao, J.P. Stegemann, Delivery of mesenchymal stem cells in chitosan/collagen microbeads for orthopedic tissue repair. Cells Tissues Organs **197**, 333 (2013). https://doi.org/10.1159/000348359

G. Wang, D. Chen, L. Zhang, et al., A mild route to entrap papain into cross-linked PEG microparticles via visible light-induced inverse emulsion polymerization. J. Mater. Sci. **53**, 880 (2018). https://doi.org/10.1007/s10853-017-1484-9

U. Wattendorf, G. Coullerez, J. Vörös, et al., Mannose-based molecular patterns on stealth microspheres for receptor-specific targeting of human antigen-presenting cells. Langmuir **24**, 11790–11802 (2008). https://doi.org/10.1021/la801085d

A.R. Wu, J.B. Hiatt, R. Lu, et al., Automated microfluidic chromatin immunoprecipitation from 2,000 cells. Lab Chip **9**, 1365–1370 (2009). https://doi.org/10.1039/b819648f

Y. Xia, D.W. Pack, Uniform biodegradable microparticle systems for controlled release. Chem. Eng. Sci. **125**, 129–143 (2015). https://doi.org/10.1016/J.CES.2014.06.049

F. Xu, C.M. Wu, V. Rengarajan, et al., Three-dimensional magnetic assembly of microscale hydrogels. Adv. Mater. **23**, 4254–4260 (2011). https://doi.org/10.1002/adma.201101962

X. Yan, R.A. Gemeinhart, Cisplatin delivery from poly(acrylic acid-co-methyl methacrylate) microparticles. J. Control. Release **106**, 198 (2005). https://doi.org/10.1016/j.jconrel.2005.05.005

J.O. You, D.T. Auguste, Feedback-regulated paclitaxel delivery based on poly(N,N-dimethylaminoethyl methacrylate-co-2-hydroxyethyl methacrylate) nanoparticles. Biomaterials **29**, 1950 (2008). https://doi.org/10.1016/j.biomaterials.2007.12.041

L. Zhang, K. Chen, H. Zhang, et al., Microfluidic templated multicompartment microgels for 3D encapsulation and pairing of single cells. Small **14**, 1–8 (2018). https://doi.org/10.1002/smll.201702955

R. Zilionis, J. Nainys, A. Veres, et al., Single-cell barcoding and sequencing using droplet microfluidics. Nat. Protoc. **12**, 44–73 (2017). https://doi.org/10.1038/nprot.2016.154